

MICROFLUIDIC IMPEDANCE CYTOMETER FOR CHARACTERIZATION OF SUBCELLULAR MORPHOLOGY OF SINGLE CELLS

Niels Haandbæk, Sebastian C. Bürigel, Fabian Rudolf, Flavio Heer, and Andreas Hierlemann
Dept. of Biosystems Science and Engineering, ETH Zurich, Basle, SWITZERLAND

ABSTRACT

This paper reports on a microfluidic impedance cytometer permitting dielectric characterization of single cells at frequencies up to 500 MHz. This represents a more than ten-fold frequency increase compared to other devices and enables to study both, low and high frequency dielectric properties in parallel. The increased range potentially allows for characterization of subcellular components in addition to the properties that are visible at lower frequencies, such as cell volume and membrane capacitance. We demonstrate the capabilities of the cytometer by discriminating wild-type yeast from a mutant, which differs in size and distribution of vacuoles in the intracellular fluid. The discrimination is based on the differences in dielectric properties at frequencies up to 200 MHz.

KEYWORDS

Electric impedance, flow cytometry, impedance cytometer, microfluidic device, cell differentiation, *S. cerevisiae*.

INTRODUCTION

Impedance spectroscopy is a non-invasive technique for characterizing the dielectric properties of materials and their interfaces. The technique has found use in areas, such as electrochemistry [1] and materials science [2], where it is used to study systems with solid-liquid and solid-solid interfaces. Examples of applications include the characterization of fuel cells [3], rechargeable batteries [4], and corrosion phenomena [5]. It has recently also gained relevance for the characterization of biological tissues and cells, as reviewed in [6]. The dielectric properties of cells reveal information on membrane resistance, membrane capacitance and cytoplasmic conductivity at frequencies below 10 MHz [7]. However, the investigation of subcellular components, such as vacuoles, can only be performed at much higher frequencies [8].

Typically, cells have been characterized using bulk suspensions [9], and the results, therefore, represent a population average [10]. A population average does not reveal important details of heterogeneity of individual cells, details, which are needed to develop mathematical descriptions of cellular behavior [11]. Analysis techniques with single-cell resolution have, therefore, become increasingly important to address such questions [12].

The combination of impedance spectroscopy with a microfluidic flow cytometer results in a lab-on-chip device, capable of label-free impedance characterization of single cells [14]. Cells or particles are dispersed in a liquid, typically an electrolyte, such as phosphate-buffered saline (PBS), and pumped through a microfluidic channel. The channel has two pairs of planar electrodes patterned

at the top and bottom. An impedance spectroscopy applies an AC voltage to the electrodes, which causes a current to flow between them. The current change upon passage of a cell or particle between the electrodes is differentially measured and then analyzed to determine the dielectric properties.

Hoffman et al. demonstrated a flow cytometer, capable of detecting both, low and high frequency impedance changes produced by single cells traversing a sensing orifice [13]. They introduced the concept of opacity as the ratio of the impedance magnitude at a high frequency to that at a low frequency. This is useful for normalizing the data for cell size and position between the measurement electrodes as shown by Gawad et al. [15]. They demonstrated impedance measurements of single cells using a microfluidic device with coplanar electrodes. Their investigations of the influence of different cell properties on the impedance showed that the cell size contributes to the response at all frequencies, the membrane capacitance at frequencies around 1 MHz, and the cytoplasm conductivity at frequencies approaching 10 MHz. An improved device with parallel facing electrodes was used by Cheung et al. to discriminate beads from red blood cells, red blood cells fixed using glutaraldehyde, and red-blood-cell ghosts [16]. They analyzed the impedance spectrum at two frequencies simultaneously, and found a difference in opacity between normal and fixed red blood cells, as well as a difference in phase between normal cells and ghosts. Schade-Kampmann et al. used an impedance device for discriminating different cell types, as well as for analyzing viability and apoptosis of Jurkat cells [17]. Holmes et al. used the method for discriminating different leukocytes in human blood [18]. They were able to make a differential white blood cell count with results that correlated well to those of commercial blood analyzers. Impedance work of other authors has been reviewed by Sun et al. [19].

In this paper, we report on a novel microfluidic impedance cytometer that covers a frequency range from DC to up to 500 MHz. The increased frequency range will allow for characterization of subcellular components, such as vacuoles and cell nuclei, in addition to the properties detectable at lower frequencies. The cytometer consists of a custom-built impedance spectroscopy, combined with a simple microfluidic device with parallel facing electrodes. The impedance spectroscopy is based on a flexible FPGA platform, which interfaces to the microfluidic device and features high-speed data converters and a trans-impedance amplifier, built from off-the-shelf components. We demonstrate the capabilities of the cytometer by discriminating wild-type yeast cells from that of a mutant, which differs in size and distribution of vacuoles. The discrimination is based on the difference in dielectric properties at frequencies up to 200 MHz.

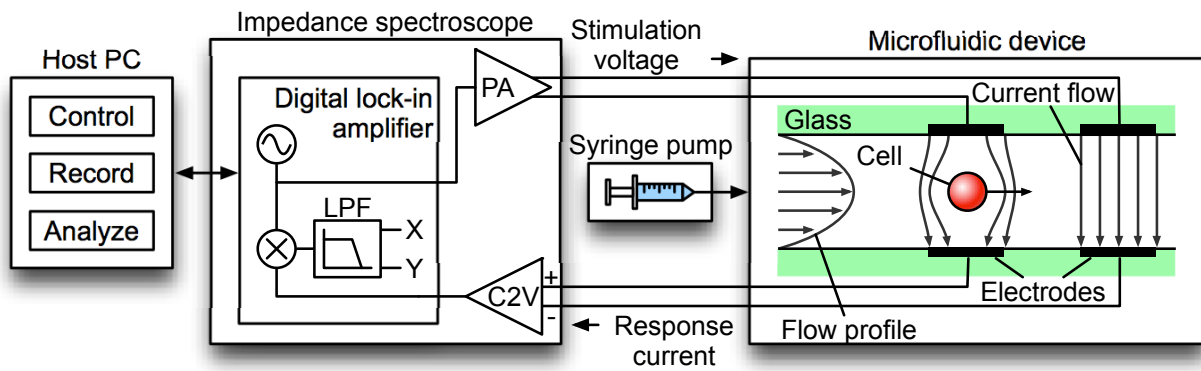


Figure 1: Schematic showing the complete microfluidic impedance cytometer. A power amplifier (PA) buffers the signal from the impedance spectroscopie, and a trans-impedance amplifier (C2V) converts the response current into a voltage. The microfluidic configuration is shown as a side view of the sensing region.

MATERIALS AND METHODS

Figure 1 shows a schematic diagram of the complete microfluidic impedance cytometer, which consists of an impedance spectroscopie, combined with a microfluidic device.

The impedance spectroscopie is based on a digital lock-in amplifier (Figure 2a), which generates the stimulation voltage and analyses the response current. The lock-in amplifier is interfaced to the analog domain by using high-speed data converters operating at 1.8 GSamples/s. The power amplifier (Figure 2b), the trans-impedance amplifier (Figure 2c) and the microfluidic device are all accommodated on a dedicated printed circuit board. This keeps the connections between the components short, which minimizes signal reflections and noise coupling into the system. The power amplifier is necessary because of the mismatch between the frequency-dependent impedance of the microfluidic channel, and the output impedance of the digital-to-analog converter (DAC). It has an input impedance of 50 Ω , which matches that of the DAC, and its close placement to the microfluidic device ensures that the signal integrity is preserved over the entire frequency range. The task of the trans-impedance amplifier is to convert the differential response current into a voltage, which can be measured by

the analog-to-digital converter (ADC).

The digital lock-in amplifier is implemented on a Xilinx Virtex-6 FPGA (Xilinx, Inc., USA). It enables generation and analysis of up to four frequencies in parallel by means of four demodulators. Each demodulator has a digitally controlled oscillator (DCO), a frequency mixer (MIX), and two low-pass filters (LPF). The lock-in amplifier output constitutes of a linear combination of the in-phase part of the signals of the four DCOs. Each DCO generates a sinusoidal carrier signal with a frequency, f_{dco} , of up to 500 MHz and a resolution of better than 10 μ Hz. The mixer shifts the frequencies of the input signal, f_{in} , to $f_{in} - f_{dco}$ and $f_{in} + f_{dco}$. The low-pass filters suppress the frequency components at $f_{in} + f_{dco}$, but also help to reject noise on the input signal. They feature configurable-order bandwidth and configurable down-sampling ratio to enable a flexible trade-off between noise rejection and response time. The samples of the resulting in-phase (X) and 90° out-of-phase (Y) signals are continuously buffered in the memory, packed in User Datagram Protocol packets and streamed to the host PC over Ethernet. Here, they are stored for off-line analysis. The lock-in amplifier can reliably deliver samples at a total sampling rate of up to 1.6 MSamples/s, shared between the four demodulators.

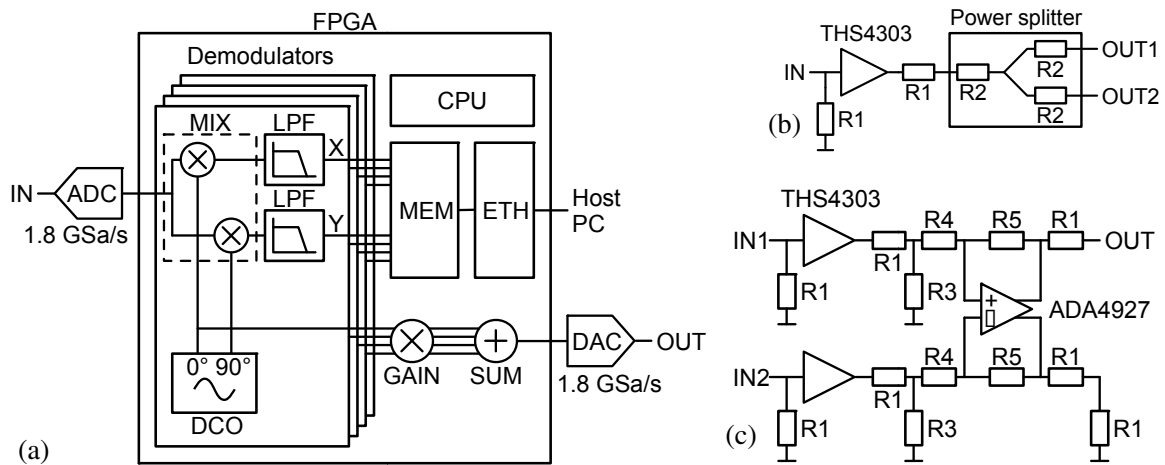


Figure 2: (a) Block diagram of the digital lock-in amplifier featuring four parallel demodulators, the outputs of which are buffered in a memory (MEM) and transmitted continuously to the host PC via Ethernet (ETH). (b) Schematic diagram of the PA featuring a gain of 5 from input to each of the outputs. (c) Schematic diagram of the C2V featuring a gain of 7.8 from input to output. The resistances R1 to R5 are 50 Ω , 16.7 Ω , 56 Ω , 301 Ω and 470 Ω , respectively.

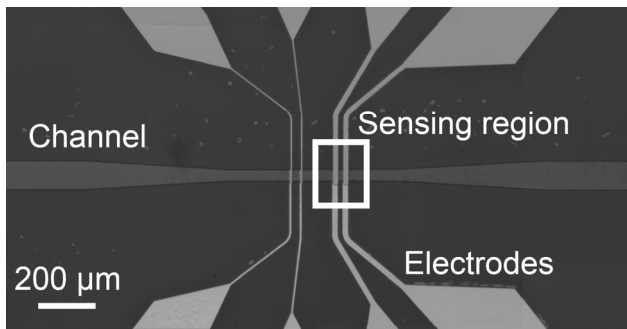


Figure 3: Micrograph of the microfluidic device. The electrodes are 18 μm wide with a center-to-center spacing of 36 μm . Channel width is 40 μm in the sensing region.

The microfluidic device (Figure 3) has been fabricated as described in [20]. It consists of two glass plates with 200-nm-thick and 18- μm -wide platinum electrodes. The two plates are bonded face to face using a 10- μm -thick lithographically structured layer of SU-8 3000 as spacer that defines the channel dimensions. The final channel cross-section in the sensing region is $40 \times 10 \mu\text{m}^2$.

Two different strains of yeast cells (*S. cerevisiae*, Euroscarf) were used: a B4741 wild-type strain, which has 1 to 4 normal-size vacuoles, and a B4741 *vac8 Δ ::kanMX* strain, which has 2 to 10 small vacuoles. Cells of each strain were separately dispersed in PBS together with 5- μm polystyrene beads (Life Technologies Ltd, UK) and driven through the channel in the microfluidic device by means of a neMESYS syringe pump (Cetoni GmbH, Germany) at a flow rate of 2 $\mu\text{l}/\text{min}$.

The impedance was analyzed within a frequency range between 500 kHz and 200 MHz. The time-domain signals from the lock-in amplifier were recorded using custom software (Zurich Instruments AG, Switzerland). The complex peak-to-peak voltage signals of beads and cells were then extracted using MATLAB (MathWorks, Inc., USA). Opacity values were calculated by normalizing the results at each frequency with the cell volume measured at 500 kHz.

RESULTS AND DISCUSSION

The opacity magnitude spectrum (Figure 4a) shows relatively constant values for the beads at all frequencies. This indicates that their impedance, compared to the surrounding medium, is independent of the frequency, which is expected, since beads consist of a uniform low-conductivity material. In contrast, the opacity of the cells decreases with increasing frequency as a consequence of their complex internal structure, which includes organelles, such as nucleus and vacuoles that are separated from the cytoplasm by membranes. Membrane capacitances become increasingly transparent with increasing frequency so that the high-conductivity media of the cytoplasm and, at higher frequencies, of the organelles contribute to the dielectric properties. A discrimination of the two yeast strains becomes possible at frequencies beyond 50 MHz, as a consequence of the presence of larger vacuoles in wild-type cells. Vacuoles have a large concentration of charged proteins and

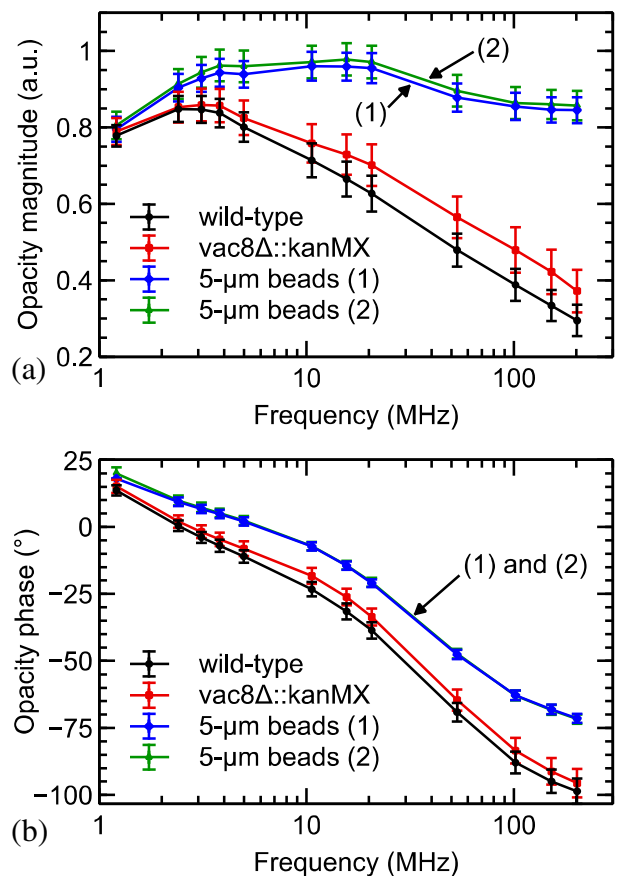


Figure 4: (a) Opacity magnitude spectrum for the two yeast strains, wild-type and *vac8 Δ ::kanMX*, as well as 5- μm beads. The beads were measured together with the wild-type (1) and *vac8 Δ ::kanMX* strains (2). The two strains only differ in subcellular features, i.e., the number and size of vacuoles, and can, therefore, only be discriminated at frequencies higher than 50 MHz. (b) Opacity phase spectrum for the two yeast strains, wild-type and *vac8 Δ ::kanMX*, as well as 5- μm beads. The results show that the phase information alone is insufficient to discriminate the two strains at any applied frequency.

feature, therefore, higher conductivity values, which results in lower opacity values. The opacity phase spectrum (Figure 4b) also shows a difference between the two strains. The wild type shows a slightly larger phase shift, due to a larger capacitance, which is, however, not pronounced enough for reliable discrimination.

CONCLUSIONS

We have presented a novel microfluidic impedance cytometer, capable of simultaneous analysis at four frequencies between DC and 500 MHz. This represents a more than ten-fold increase in the frequency range in comparison to other devices. We have demonstrated that the instrument can measure relevant impedance characteristics for single cells as well as for beads up to a frequency of at least 200 MHz. We have shown that it is possible to discriminate between wild-type yeast and a mutant strain, which differs only in subcellular morphology, namely the size and distribution of vacuoles. The discrimination was based on opacity values at

frequencies above 50 MHz.

Current work includes the use of the high frequency capabilities of the cytometer to characterize yeast cells with other mutations that affect their subcellular morphology.

ACKNOWLEDGEMENTS

The research leading to these results has received funding from the Commission for Technology and Innovation, CTI, Switzerland under project no. 11174.2 PFLS-LS.

REFERENCES

- [1] E. Barsoukov and J. R. Macdonald, Eds., *Impedance Spectroscopy*, John Wiley & Sons, Inc., 2005.
- [2] D. Raistrick, "Application of Impedance Spectroscopy to Materials Science", *Annual Review of Materials Science*, vol. 16, pp. 343–370, 1986.
- [3] W. Vielstich, A. Lamm, H. A. Gasteiger, and H. Yokokawa, Eds., *Handbook of Fuel Cells*, John Wiley & Sons, Ltd, 2010.
- [4] B. V. Ratnakumar, M. C. Smart, and S. Surampudi, "Electrochemical impedance spectroscopy and its applications to lithium ion cells," in *Proceedings of the Seventeenth Annual Battery Conference on Applications and Advances*, Long Beach, January 15–18, 2002, pp. 273–277.
- [5] A. Nishikata, Y. Ichihara, and T. Tsuru, "Electrochemical impedance spectroscopy of metals covered with a thin electrolyte layer," *Electrochimica Acta*, vol. 41, no. 7–8, pp. 1057–1062, 1996.
- [6] K. R. Foster and H. P. Schwan, "Dielectric properties of tissues and biological materials: a critical review.", *Critical reviews in biomedical engineering*, vol. 17, pp. 25–104, 1989.
- [7] R. Pethig and D. B. Kell, "The passive electrical properties of biological systems: their significance in physiology, biophysics and biotechnology", *Physics in Medicine and Biology*, vol. 32, pp. 933–970, 1987.
- [8] K. Asami, T. Yonezawa, "Dielectric behavior of wild-type yeast and vacuole-deficient mutant over a frequency range of 10 kHz to 10 GHz.", *Biophysical journal*, vol. 71, pp. 2192–200, 1996.
- [9] C. M. Harris, R. W. Todd, S. J. Bungard, R. W. Lovitt, J. G. Morris, and D. B. Kell, "Dielectric permittivity of microbial suspensions at radio frequencies: a novel method for the real-time estimation of microbial biomass," *Enzyme and Microbial Technology*, vol. 9, no. 3, pp. 181–186, 1987.
- [10] D. Di Carlo and L. P. Lee, "Dynamic Single-Cell Analysis for Quantitative Biology", *Analytical Chemistry*, vol. 78, pp. 7918–7925, 2006.
- [11] M. E. Lidstrom and D. R. Meldrum, "Life-on-a-chip.", *Nature reviews. Microbiology*, vol. 1, pp. 158–64, 2003.
- [12] H. A. Svahn and A. van den Berg, "Single cells or large populations?", *Lab on a chip*, vol. 7, pp. 544–6, 2007.
- [13] R. A. Hoffman, T. S. Johnson, and W. B. Britt, "Flow cytometric electronic direct current volume and radiofrequency impedance measurements of single cells and particles.," *Cytometry*, vol. 1, no. 6, pp. 377–84, 1981.
- [14] S. Gawad, L. Schild, and P. H. Renaud, "Micromachined impedance spectroscopy flow cytometer for cell analysis and particle sizing.", *Lab on a chip*, vol. 1, pp. 76–82, 2001.
- [15] S. Gawad, K. Cheung, U. Seger, A. Bertsch, and P. Renaud, "Dielectric spectroscopy in a micromachined flow cytometer: theoretical and practical considerations.", *Lab on a chip*, vol. 4, pp. 241–51, 2004.
- [16] K. Cheung, S. Gawad, and P. Renaud, "Impedance spectroscopy flow cytometry: on-chip label-free cell differentiation", *Cytometry. Part A*: *the journal of the International Society for Analytical Cytology*, vol. 65, 124–32, 2005.
- [17] G. Schade-Kampmann, a Huwiler, M. Hebeisen, T. Hessler, and M. Di Berardino, "On-chip non-invasive and label-free cell discrimination by impedance spectroscopy.", *Cell proliferation*, vol. 41, pp. 830–40, 2008.
- [18] D. Holmes, D. Pettigrew, C. H. Reccius, J. D. Gwyer, C. van Berkel, J. Holloway, D. E. Davies, and H. Morgan, "Leukocyte analysis and differentiation using high speed microfluidic single cell impedance cytometry.", *Lab on a chip*, vol. 9, pp. 2881–2889, 2009.
- [19] T. Sun, H. Morgan, "Single-cell microfluidic impedance cytometry: a review", *Microfluidics and Nanofluidics*, vol. 8, pp. 423–443, 2010.
- [20] S. C. Bürgel, Z. Zhu, N. Haandbaek, O. Frey, and A. Hierlemann, "Dynamic and static impedance spectroscopy for single particle characterization in microfluidic chips", in *2012 IEEE 25th International Conference on Micro Electro Mechanical Systems (MEMS)*, pp. 1033–1036, 2012.

CONTACT

N. Haandbæk, tel: +41-61-387-3183;

niels.haandbaek@bsse.ethz.ch